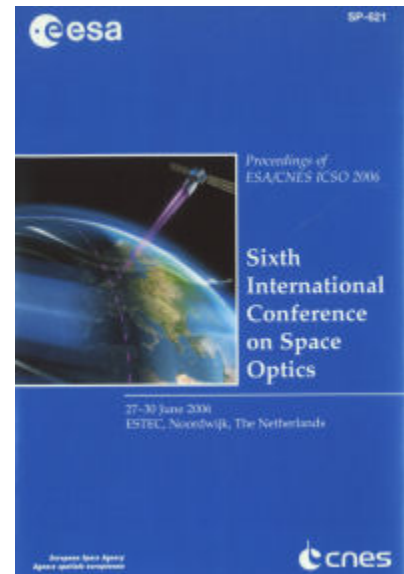


International Conference on Space Optics—ICSO 2006

Noordwijk, Netherlands

27–30 June 2006

Edited by Errico Armandillo, Josiane Costeraste, and Nikos Karafolas



Optical metrology subsystem of the LISA gravitational wave detector

Dennis Weise, Claus Braxmaier, Peter Gath, Hans Reiner Schulte, et al.



OPTICAL METROLOGY SUBSYSTEM OF THE LISA GRAVITATIONAL WAVE DETECTOR

Dennis Weise¹, Claus Braxmaier^{1,2}, Peter Gath¹, Hans Reiner Schulte¹, and Ulrich Johann¹

¹*EADS Astrium GmbH, 88039 Friedrichshafen, Germany, e-mail: dennis.weise@astrium.eads.net*

²*Hochschule für Technik, Wirtschaft & Gestaltung, Braunergerstr. 55, 78462 Konstanz, Germany, e-mail: braxm@fh-konstanz.de*

ABSTRACT

We present a detailed concept for the realization of the LISA optical metrology subsystem, which employs heterodyne interferometry in a so-called “strap-down” architecture to accomplish a highly sensitive detection of gravity-wave induced displacements of dedicated mass references within the payload of the three LISA satellites. A frequency swap between transmitted and local reference beam is introduced to minimize the impact of stray light on the measurement sensitivity. The performance of the system is demonstrated by first optical modeling.

1. INTRODUCTION

The joint ESA/NASA mission LISA (Laser Interferometer Space Antenna) aims at detecting gravitational waves from astrophysical objects and events in the frequency range 30 μ Hz to 1 Hz. It will be implemented in a constellation of three identical spacecraft at the corners of an equilateral triangle with a 5 million kilometer arm length, which is trailing earth in a heliocentric orbit. Each spacecraft carries a payload with two free-falling “proof masses” defining the end points of the individual arms. The passage of a gravitational wave will cause minute changes in the distance between the two proof masses of each arm, which are observed by the LISA optical metrology subsystem through laser interferometry, which mutually links the three spacecraft in an active transponder scheme.

The precision required for the detection of proof mass displacements is given in terms of the so-called strain sensitivity $h = 2 \delta L/L$, for which a noise level below 3.2×10^{-19} at a frequency of 1 mHz has to be provided. The detection sensitivity is limited by residual proof mass accelerations from disturbance forces at low frequencies (below 3 mHz), and optical metrology noise at high frequencies (above 3 mHz). For the

latter, a total budget of approx.

$$12 \frac{\text{pm}}{\sqrt{\text{Hz}}} \times \sqrt{1 + \left(\frac{2.8 \text{ mHz}}{f}\right)^4} \quad (1)$$

is currently allocated per laser link, which includes all associated contributions such as shot noise, laser phase noise, and geometrical projection effects.

The accurate determination of arm length variations is complicated by the fact that the shape of the formation triangle undergoes residual seasonal changes, which cannot be completely removed by orbit optimization. These changes not only affect the nominal 60° angle between the lines of sight, but also the so called point-ahead angle, which describes the offset between received and transmitted beam for each individual spacecraft. This offset is required to account for the comparatively long travel time of the laser light to the respective remote spacecraft, which is calculated to be approx. 16.7 s. An active compensation has to be foreseen for the variation of the angle between the lines of sight ($\pm 1^\circ$) and the out-of-plane point-ahead angle ($\pm 6 \mu\text{rad}$).

The combination of picometer resolution, a transmission path of 5 Mio. km, and the need for active elements in the optical science chain leads to an exceptional engineering challenge for the realization of the LISA payload and the metrology system in particular. Here, we present a detailed concept for the opto-mechanical design, developed in the context of the ESA funded LISA Mission Formulation Study currently led by EADS Astrium.

2. PAYLOAD DESIGN

An overview of the optical part of the payload within each of the LISA satellites is given in Figure 1. It consists of two so-called “movable optical assemblies”, each pointing to its remote counterpart located in the satellites at the other two corners of the constellation triangle. The nominal 60° angle between the assemblies can be varied with the help of

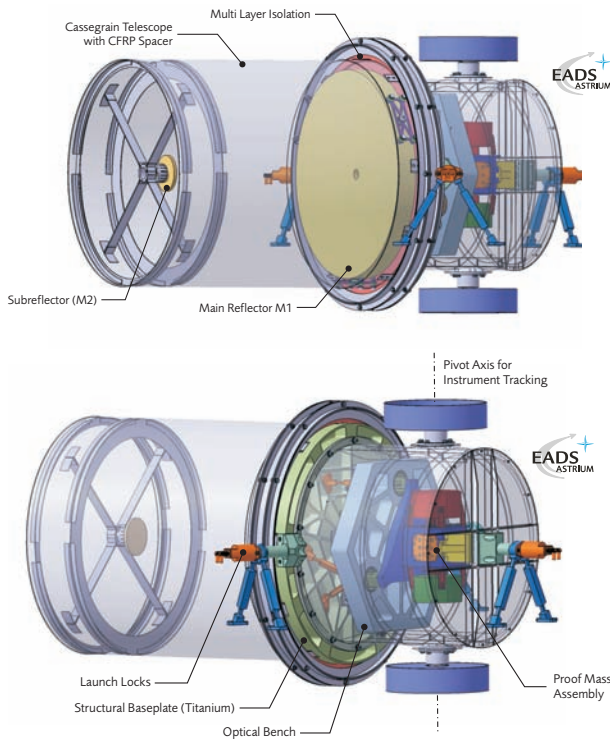


Figure 1. Movable optical assembly within the LISA payload. Each spacecraft contains two of these assemblies, each pointing to its respective remote counterpart under a 60° angle.

an ultra low noise tracking mechanism that rotates each assembly in total around a pivot axis running through the center of its associated proof mass.

The Au-Pt proof mass cube, whose gold-plated front surface acts as an active mirror in the optical metrology system, is engaged in an electrode housing for electrostatic sensing and actuation, which is supported by a dedicated titanium structure. Furthermore, the movable assemblies comprise a Cassegrain telescope and an optical bench as main optical subsystems. The Cassegrain telescope is characterized by an aperture diameter of 400 mm, a system focal length of 4800 mm, and a comparatively large magnification of 80. Main reflector M1 and subreflector M2 are separated by 450 mm with the help of a CFRP tube spacer. The telescope ocular is located on the optical bench, whose plane is oriented normal to the telescope axis. Here, a pupil of 5 mm diameter is provided, in which a “Point-Ahead Angle Mechanism” can be placed for the correction of the out-of-plane point-ahead angle. Both the transmitted and the received for each optical assembly are processed with the same telescope.

The optical bench is the heart of the LISA metrology system and contains all interferometers with their corresponding photodiodes as well as additional optics and detectors for power stabilization, initial beam acquisition etc. Like the telescope mirrors, it

is made from ultra low expansion glass (Zerodur) to minimize thermo-elastic deformations. It is mechanically supported by three isostatic mounts interfacing a structural titanium baseplate between optical bench and telescope. The connection to the proof mass assembly is realized such that the optical bench is maximally decoupled from any external loads.

3. METROLOGY CONCEPTS

Apart from the development of an efficient scheme for canceling laser phase noise on several levels, crucial for ensuring the feasibility of LISA has been the introduction of advanced metrological concepts for accomplishing the inter-spacecraft interferometry. Main opto-mechanical payload features are:

- Polarizing heterodyne interferometry
- Differential wavefront sensing
- Strap-down architecture with optical readout (two-step interferometry)
- Frequency swap between transmit and local oscillator beam

These will be explained in the following.

3.1. Polarizing Heterodyne Interferometry

The proposed payload architecture employs heterodyne interferometry as main metrology principle. It is characterized by a frequency offset between reference and measurement beam, which allows for pure AC phase detection, ideally insensitive to intensity fluctuations. In case of LISA, the heterodyne frequency is determined by the Doppler shift of the received beam, which will be on the order of 20 MHz.

A passing gravitational wave will induce a slight phase shift in the measurement beam over the 5 million kilometer distance, which can be detected with extremely high sensitivity ($\sim 10^{-5} \text{ rad}/\sqrt{\text{Hz}}$) by sophisticated signal (phasemeter) processing. Depending on the algorithmic combination of the available signals from the various interferometers in the complete LISA constellation, several types of interferometers can be synthesized, such as Michelson or Sagnac types.

For optical beam multiplexing, polarization sensitive elements (such as polarizing beam splitters and waveplates) are utilized. This allows for a high suppression of mixing between the transmitted and the received beam, as well as the possibility to arrange for normal incidence on the proof mass in the optical readout, which simplifies beam routing and avoids coupling of longitudinal proof mass movements to lateral beam steering.

3.2. Differential Wavefront Sensing

As for the LISA Technology Package on LISA Pathfinder [1], differential wavefront sensing [2, 3] is employed to derive information on the wavefront tilt of the measurement beam with respect to the reference beam in addition to the detection of longitudinal phase shifts. This is accomplished by combining heterodyne interferometry with a spatially resolved phase measurement through the use of quadrant photodiodes. The signals obtained from the individual quadrants show relative phase shifts, depending on the spatial variation of the phase difference between reference and measurement beam, from which the relative wavefront tilt can be inferred with nrad resolution.

In the LISA payload concept presented here, differential wavefront sensing (DWS) is applied both for precision sensing of the payload attitude with respect to the line of sight to the remote spacecraft, as well as for an optical readout of 2 rotational degrees of freedom of the proof mass with respect to the optical bench. The first task is realized by the use of DWS on the science photodiodes, which is essential to reject projection effects in the distance metrology by sufficient pointing knowledge. The use of DWS in the optical readout of the proof mass is of benefit for the Drag-Free and Attitude Control System (DFACS), which can thus be provided with attitude information at an accuracy not achievable with the electrostatic readout.

3.3. Strap-Down Architecture

The metrology chain in the current payload design is characterized by a “strap-down” architecture, which introduces a technical and functional decoupling of the proof mass assembly from the intra-spacecraft interferometry. The measurement is separated into two steps, where one set of interferometers measures the path length changes from optical bench to optical bench, and a second set of interferometers measures the movement of each proof-mass with respect to each corresponding optical bench (Figure 2). The actual science measurement is then derived on the basis of the thermal and dimensional stability of each optical bench.

The additional interferometer required in the strap-down design for sensing of proof-mass movements with respect to the associated optical bench introduces the concept of an “optical readout” (ORO) into the metrology scheme. While the strap-down approach absolutely requires an optical readout for the detection of proof mass movements along the external line of sight with science precision (compare Equation (1)), additional OROs are conceivable for further proof mass degrees of freedom for DFACS support, as already indicated above. These could

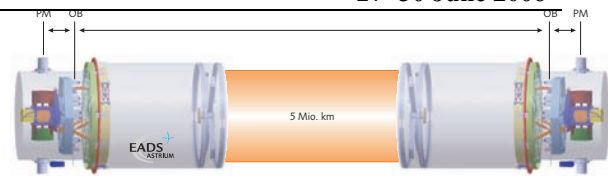


Figure 2. Strap-down principle. The proof-mass to proof-mass metrology is separated into two steps, which are referenced to the two optical benches and correlated via their thermo-elastic stability.

either be implemented in redundancy to or even in replacement for the electrostatic readout.

3.4. Frequency Swap

Of special concern for LISA is the impact of stray light on the measurement noise, as the optical power in the received beam will be more than 9 orders of magnitude below that of the transmitted beam, while both are processed with the same telescope. Stray light from the transmit beam is particularly harmful if a local oscillator with identical frequency is utilized for the science heterodyne detection. Therefore, an additional frequency offset between transmit and local oscillator beam is introduced. This can be realized in a straightforward manner by sharing part of the light of the two transmit beams per spacecraft between the two optical benches and operating the respective lasers at slightly different frequencies, as illustrated in Figure 3 (“frequency swap”).

In consequence, the following beat signals are measured on the two optical benches of each spacecraft:

- Optical bench 1
 - Science measurement:
Science 1 (signal) – LO2 (reference)
 - PM optical readout:
LO1 (signal) – LO2 (reference)
 - Phase compensation:
LO1 – LO2
- Optical bench 2
 - Science measurement:
Science 2 (signal) – LO1 (reference)
 - PM optical readout:
LO2 (signal) – LO1 (reference)
 - Phase compensation:
LO1 – LO2

The two phase compensation signals obtained on the optical benches not only represent the reference for demodulation of the measurement signals, but are also used for phase locking of the two active lasers in

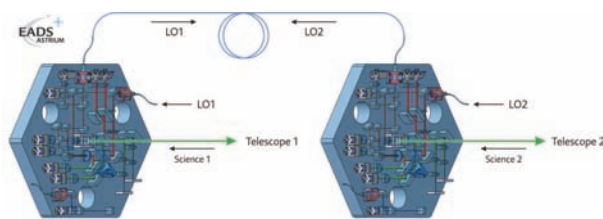


Figure 3. Frequency swap concept. A single fiber link between the two optical benches of each spacecraft is used to exchange the individual transmit frequencies between them.

each spacecraft. Therefore, a constant phase relation has to be ensured between the two corresponding interferometers. A common mode rejection of phase shifts introduced by the fiber link between the optical benches is achieved by exchanging LO1 and LO2 with equal polarizations in a single fiber.

4. OPTICAL DESIGN

The above metrology principles have been translated into a detailed optical layout for the LISA interferometric measurement system, including appropriate imaging optics. The layout is currently being analyzed with a specialized optics code (BeamWarrior [4]). First results will be presented below.

4.1. Optical Bench Layout

The optical bench is a light-weighted Zerodur hexagon with a thickness of 40 mm and a diameter of 340 mm. It is held within the payload compartment near room temperature at a temperature stability of $\sim 10^{-5} \text{ K}/\sqrt{\text{Hz}}$ to ensure the required dimensional stability between the attached optical elements. These are assumed to be made from Fused Silica and rigidly mounted by hydroxide catalysis bonding [5].

The layout of the optical bench is illustrated in Figure 4. Its optical interface to the Cassegrain telescope as well as to the proof mass is a common folding mirror, which is used on both surfaces such that the corresponding beam axes both coincide with the external line of sight. The optical bench contains three interferometers, in consistence with the measurement principles described above: the main science interferometer, the optical readout interferometer, and the reference interferometer. Additional detectors are power monitor diodes for the transmit beam and redundant CCDs for initial acquisition of the incident beam from the remote spacecraft. Also, a possible reference cavity is shown which can be used for frequency pre-stabilization of the utilized laser systems (compare [6]).

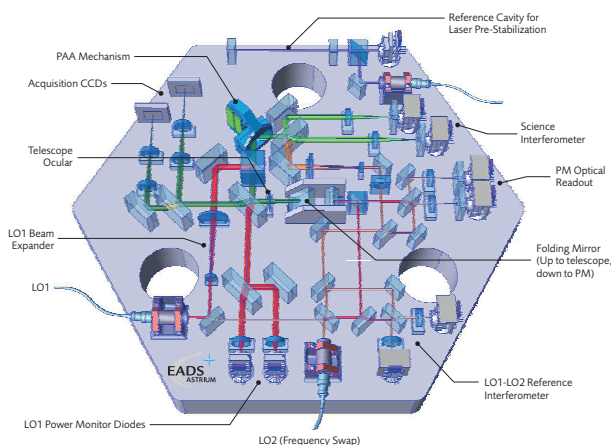


Figure 4. Interferometric layout of the optical bench.

The optical bench is fed at the “LO1” fiber launcher from a fiber-amplified Nd:YAG NPRO laser system [6], which has to deliver a power of roughly 700 mW at the fiber launcher output. A small fraction of this light passes a first beam splitter and is made available for local interferometry and the frequency swap. Most of the light is however reflected from this beam splitter and directly goes into the transmission path to the remote spacecraft. A beam expander first provides a mode-matching ensuring proper imaging of the new waist position into the exit pupil of the telescope. The transmit path is then combined with that of the received beam using a polarizing beam splitter. In the region common to both beams, the chosen setup arranges for perpendicular polarizations, such that any back reflections of the transmit beam do not leak into the receive path after demultiplexing. Before injection into the telescope, the power of the transmit beam is monitored with dedicated, redundant photodiodes, which provide the possibility for power stabilization feedback to the associated laser system.

For initial acquisition in the early mission phase when the attitude knowledge is still inaccurate, a small part of the received beam is first directed onto CCD sensors after the telescope ocular. Here, specially tailored imaging optics provide an external field of view of more than $\pm 250 \mu\text{rad}$. Once initial acquisition is accomplished, precision attitude information is obtained by DWS on the science photodiodes, as explained above. After demultiplexing of transmit and receive beams at the common polarizing beam splitter, the out-of-plane point-ahead angle is corrected by an ultra low noise Gimbal mechanism (“Point-Ahead Angle Mechanism”). Subsequently, the receive beam is combined with the “LO2” beam from the other optical bench for science interferometry. Both the Point-Ahead Angle Mechanism and the science photodiodes are located in pupil planes, in order to ensure pure angle correction and sensing, respectively, without lateral beam shifts.

The optical readout of the proof mass for one longitudinal and two rotational degrees of freedom is realized by using the LO1 beam as measurement beam, where the proof mass reflection is separated from the incident light by a the combination of a polarizing beam splitter and a quarter waveplate. Again, proof mass surface and the ORO photodiodes are located in respective image planes to minimize beam walking effects for non-zero tilt angles of the proof mass.

4.2. Optical Performance

The optical modeling of the current layout has so far been focused on the far field quality of the transmitted laser beam as well as the imaging of the received beam from the telescope aperture to the science photodiodes. Additionally, the optical performance of the acquisition CCDs has been verified and a first assessment of misalignment sensitivities has been performed.

For a calculation of the far field intensity and phase distribution, the simulation started from a Gaussian beam with a waist radius of 1 mm located on the

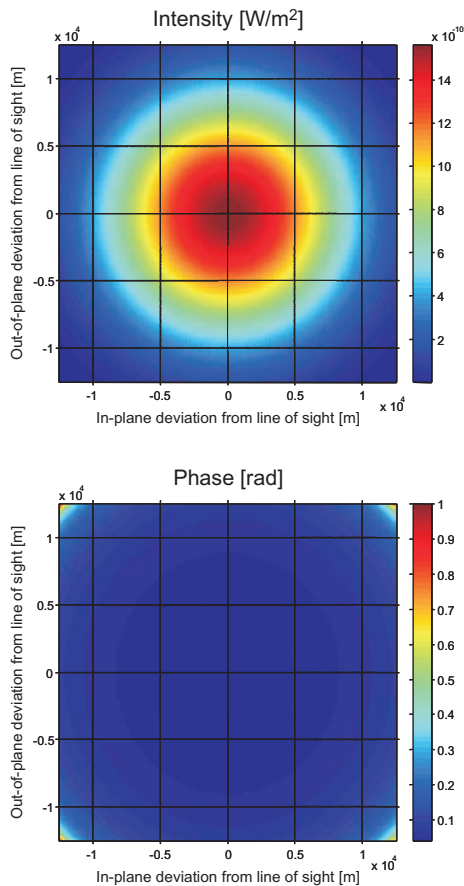


Figure 5. Simulated far field intensity and phase on a 5 Mio. km sphere, centered in the exit pupil of the telescope.

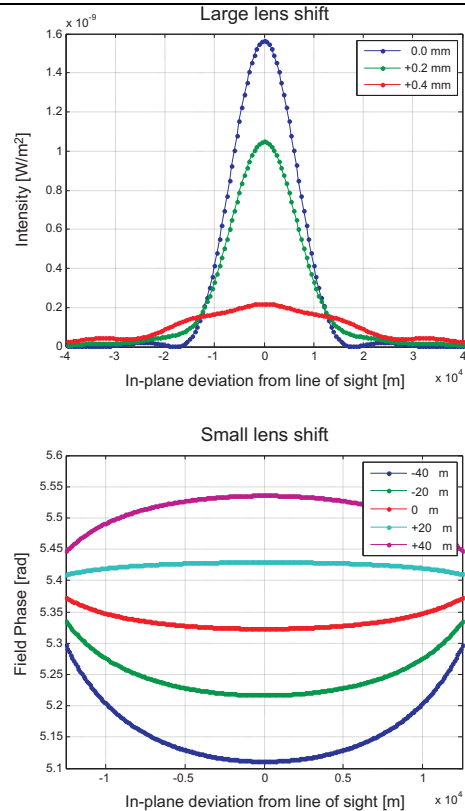


Figure 6. Far field shaping by active adjustment of the first beam expander lens on the optical bench.

first beam splitter after the LO1 fiber launcher. The propagation into the far field accounts for all effects from optical bench components, the telescope and exit pupil clipping, resulting in the field maps shown in Figure 5. These are plotted on the surface of a sphere with a 5 Mio. km radius, centered in the aperture of the telescope. Of importance for LISA is in particular a flat phase in the vicinity of the line of sight to avoid coupling of spacecraft pointing jitter to phase jitter.

As illustrated in Figure 6, the far field shape, both in intensity and phase, can be fine-tuned by a longitudinal shift of the first beam expander lens in the transmit path. This can be used to correct for residual wavefront curvatures from non-optimal alignment of imaging optics (phase plot), as well as for an expansion of the far field cone (intensity plot), which might aid beam search in case the laser link is lost.

To verify the receive beam path, an ideal plane wavefront is propagated from the telescope entrance pupil through the optical system. Any wavefront tilts are linearly mapped into unambiguous positions on the acquisition CCDs, as illustrated in Figure 7. The imaging system has been optimized for a CCD surface of approx. 12×12 mm. On the science photodiodes with an assumed diameter of 0.5 mm, slight aberrations are visible (Figure 8) even in the nominal

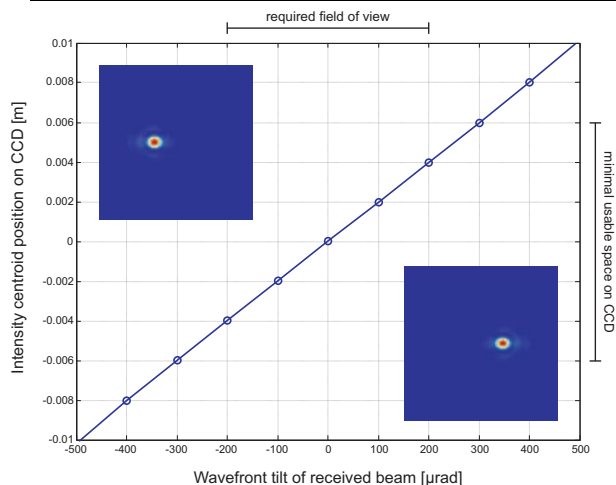


Figure 7. Conversion of wavefront tilt into lateral shift of the intensity centroid on the acquisition CCDs.

case without wavefront tilt. Nonetheless, a heterodyne efficiency of about 85 % is achieved by overlapping a Gaussian local oscillator beam shape, whose diameter is 5 mm before the final beam compressor in front of the science photodiodes.

5. SUMMARY AND OUTLOOK

In summary, we have presented a detailed concept for the interferometric measurement system on board the LISA satellites, which should allow for a detection of gravity-wave induced path length changes with picometer sensitivity. First numerical analysis of the optical setup confirm the robustness of the architecture and give faith in the feasibility of the mission. Extensive optical modeling is on-going to further assess far field effects as well as alignment and manufacturing tolerances.

6. ACKNOWLEDGMENTS

This work was supported under ESA Contract No. 18756/04/NL/HB. The authors further thank Jan Hopman, Niek Doelman, and colleagues of TNO (Delft), Gerhard Heinzl and colleagues of the Albert-Einstein-Institute (Hannover), as well as David Robertson and colleagues of Glasgow University for their appreciated contributions.

REFERENCES

[1] G. Heinzl, C. Braxmaier, M. Caldwell, K. Danzmann, F. Draaisma, A. Garcia, J. Hough, O. Jennrich, U. Johann, C. Killow, K. Middleton, M. te Plate, D. Robertson, A. Rüdiger,

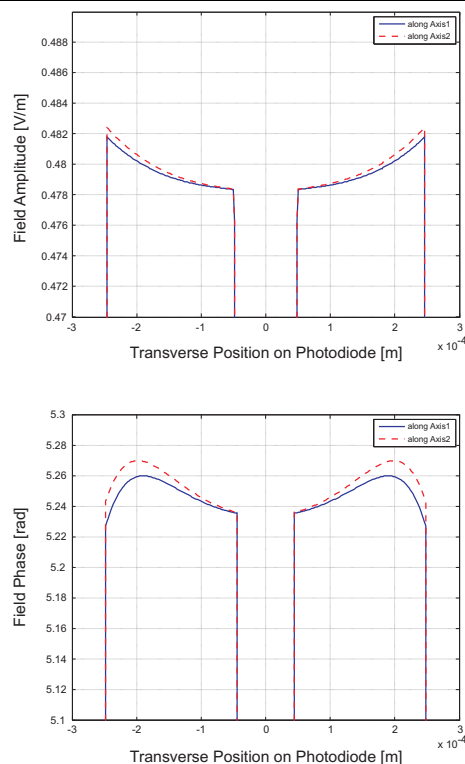


Figure 8. Field and phase cuts for the receive beam on the science photodiodes.

R. Schilling, F. Steier, V. Wand, and H. Ward. Successful testing of the LISA technology package (LTP) interferometer engineering model. *Class. Quantum Grav.*, 22:1, 2005.

[2] E. Morrison, B. J. Meers, D. I. Robertson, and H. Ward. Automatic alignment of optical interferometers. *Applied Optics*, 33(22):5041, 1994.

[3] E. Morrison, B. J. Meers, D. I. Robertson, and H. Ward. Experimental demonstration of an automatic alignment system for optical interferometers. *Applied Optics*, 33(22):5037, 1994.

[4] R. Wilhelm. *Novel numerical model for dynamic simulation of optical stellar interferometers*. PhD thesis, Technische Universität Berlin, 1999.

[5] E. J. Elliffe, J. Bogenstahl, A. Deshpande, J. Hough, C. Killow, S. Reid, D. Robertson, S. Rowan, H. Ward, and G. Cagnoli. Hydroxide-catalysis bonding for stable optical systems for space. *Class. Quantum Grav.*, 22:S257, 2005.

[6] D. Weise, J. Limpert, T. Schreiber, C. Braxmaier, C. Wührer, P. Gath, H. R. Schulte, A. Tünnermann, and U. Johann. All-fiber-coupled, master oscillator fiber power amplifier based laser assembly for the LISA gravitational wave detector. *ICSO Conference Proceedings*, 2006.